Flood-driven CO_2 emissions from adjacent North Carolina estuaries during Hurricane Joaquin (2015)

Bryce R. Van Dam[a,*], Joseph R. Crosswell[a,b], Hans W. Paerl[a]

[a] Institute of Marine Sciences, University of North Carolina at Chapel Hill, Morehead City, NC, USA
[b] CSIRO Oceans and Atmosphere, Brisbane, QLD, Australia

A B S T R A C T

Extreme climatic events like floods and hurricanes have the potential to significantly alter coastal carbon cycling. However, due to the challenges associated with sampling these events, they can be difficult to incorporate into regional and global carbon budgets. To address this data gap, we bracket a major flooding event associated with the passing of Hurricane Joaquin (October 2015) with direct and high-resolution pCO_2 measurements in the Neuse (NeuseRE) and New River Estuary (NewRE), North Carolina. Enhanced river discharge quickly flushed the relatively small NewRE, causing residence time to fall from 90 to 9 days, while the larger NeuseRE responded relatively slowly to flooding. This period of rapid flushing coincided with a significant increase in CO_2 fluxes. The effect of cooler flood-waters, which reduce pCO_2, was counteracted by allochthonous DIC inputs, which drove large increases in pCO_2 relative to dissolved O_2. The spatial distribution of carbonate buffering differed between estuaries, enhancing CO_2 fluxes in the NewRE (178 mmol C m^{-2} d^{-1}), while partially limiting air-water exchange in the NeuseRE (62 mmol C m^{-2} d^{-1}). While windy storms may drive larger CO_2 fluxes from estuaries, we show that flooding events can also contribute significantly to annual carbon budgets. CO_2 emissions during this ~14-day flood period accounted for 31% (NeuseRE) to 44% (NewRE) of the total annual CO_2 flux. Our findings show that sufficient spatial and temporal coverage during storms is necessary for estuarine CO_2 fluxes to be reliably assessed over annual or longer time scales.

1. Introduction

Estuaries play a disproportionately large role in the global C cycle. While comprising only ~0.2% of the area of the ocean, they release between 0.1 and 0.5 Pg C yr^{-1}, approaching the rate of CO_2 uptake over continental shelves (Cole et al., 2007; Bauer et al., 2013; Cai, 2011; Chen and Borges, 2009; Chen et al., 2013). These estimates are largely based on estuarine CO_2 fluxes determined at infrequent intervals and scaled to a full year. Thus, they inevitably miss short-term variability driven by episodic events like storms and droughts. At long time scales, most estuaries are CO_2 sources to the atmosphere. However, some estuaries can be CO_2 sinks when assessed on annual (Maher and Eyre, 2012) to diel (Crosswell et al., 2017) time scales. This uncertainty in the short-term spatial and Temporal variability in estuarine CO_2 emissions remains a key data gap (Zscheischler et al., 2017). Extreme events like tropical cyclones and nor'easters generally have a small to moderate impact on air-water CO_2 exchange in coastal waters (Ye et al., 2017) and the open ocean (Lévy et al., 2012), but these events (and associated flooding) may significantly affect estuarine pCO_2 through their effects on resident biogeochemical and physical processes (Crosswell et al., 2014; Evans et al., 2012; Jeffrey et al., 2016; Mørk et al., 2016). For example, floods can deliver large pulses of labile terrestrial organic carbon (OC) to estuaries (Bianchi et al., 2013; Dahal et al., 2014), which can be respired within the estuary, contributing to net ecosystem heterotrophy and pCO_2 (Osburn et al., 2012; Yao and Hu, 2017). On the contrary, if these flood waters are high in nutrients but low in organic carbon, primary production may be stimulated during and after the storm, resulting in a drawdown in pCO_2 (Fagan and Mackenzie, 2007; Drupp et al., 2011). However, if floodwaters are high in both dissolved organic carbon (DOC) and inorganic nutrients, microbial heterotrophic production as well as autotrophic primary production could be enhanced (Sarma et al., 2011). In this case, storms may affect the net metabolic state of the estuary in a manner consistent with variations in the ratio of OC to inorganic nutrient loading (Hopkinson and Vallino, 1995; Kemp et al., 1997; Herrmann et al., 2015). In turn, these shifts in net metabolism would affect pCO_2 distributions. Alternatively, increased precipitation can reduce dissolved inorganic carbon (DIC) faster than total alkalinity (TA), decreasing the air-water pCO_2 gradient and associated CO_2 fluxes. Storm-associated wind, storm surge, and intense rainfall will enhance the rate of air-water CO_2 exchange, while elevated river discharge may decrease the fresh water residence time, potentially affecting post-storm carbon exchanges (Paerl et al., 2006b; Paerl et al., 2018; Wetz and Yoskowitz, 2013).

Estimates of storm-related CO_2 fluxes from estuaries are few and highly variable, ranging from CO_2 uptake (Evans et al., 2012) to significant CO_2 degassing (Sarma et al., 2011; Crosswell et al., 2014; Hunt et al., 2014; Mørk et al., 2016), depending on storm characteristics and

* Corresponding author.
E-mail address: bvandam@fiu.edu (B.R. Van Dam).

https://doi.org/10.1016/j.marchem.2018.10.001
Received 10 January 2018; Received in revised form 20 September 2018; Accepted 2 October 2018
Available online 06 October 2018

estuarine morphology. Hurricane Irene (2011) drove large CO_2 fluxes in the Neuese River estuary, North Carolina (NC), which exceeded the annual riverine input of C by a factor of 4 (Crosswell et al., 2014), while a large storm caused the Columbia River estuary to transition rapidly from CO_2 source to sink behavior (Evans et al., 2012). In this study, we bracket a large flooding event in the fall of 2015 with direct pCO_2 measurements in the adjacent New River Estuary and Neuse River Estuary, NC. Both estuaries have been intensely monitored for decades, and a set of recent studies (Crosswell et al., 2012, 2014, 2017; Van Dam et al., 2018) serve as a backdrop for investigating the impact of storms relative to normal conditions in the present analysis. We employ a set of biogeochemical proxies to 1) estimate the impact of changing water temperatures on CO_2 emissions, 2) explore trends in DIC and TA in the context of chemical buffering, and 3) better understand the biological factors driving CO_2 dynamics.

2. Methods

2.1. Site description

The Neuse River Estuary (NeuseRE) and New River Estuary (NewRE) are shallow (< 3 m average depth), microtidal systems located in the eastern North Carolina coastal plain. The NeuseRE begins at the confluence of the Neuse and Trent Rivers near New Bern, NC, and flows into the Albemarle-Pamlico Sound, the second largest estuarine system in the US (Fig. 1). A string of barrier islands surrounds the estuary with only narrow tidal inlets, significantly dampening the exchange of water with the ocean; hence, water circulation is primarily affected by freshwater discharge, wind, and seiching (Luettich et al., 2000). The average freshwater residence time in the NeuseRE is 58 days but varies significantly between 7 and 136 days with changes in river discharge (Van Dam et al., 2018). The NeuseRE is eutrophic, with average primary production (PPR) of 200–500 gC $m^{-2} yr^{-1}$ (Boyer et al., 1993; Mallin et al., 1993), frequent phytoplankton blooms and bottom-water hypoxia (Paerl et al., 1998; Paerl et al., 2006a). The NeuseRE has been subject to decades of extensive study associated with a long-term monitoring project, the Neuse River Estuary Modeling and Monitoring program (ModMon; http://www.unc.edu/ims/neuse/modmon/). A similar water-quality monitoring program associated with the Defense Coastal Estuarine Research Program (DCERP; https://dcerp.rti.org/), provided field data for the NewRE. As with the NeuseRE, the NewRE has a history of cultural eutrophication with an average PPR of < 250 gC $m^{-2} yr^{-1}$, that places it the mesotrophic category (Anderson, personal communication; Mallin et al., 2005). Despite relatively limited flushing through the New River Inlet, which directly connects the NewRE to the ocean, the average residence time of the NewRE is slightly lower than the NeuseRE at 46 days (range 9–91 days) (Van Dam et al., 2018). Both the NeuseRE and NewRE inhabit watersheds that are largely agricultural, but the NewRE itself is immediately surrounded by the rapidly expanding city of Jacksonville, and Marine Corps Air Station Camp Lejeune (Fig. 1). The relatively small size of the NewRE watershed, along with extensive paved surfaces surrounding its tributaries, result in a very 'flashy' rainfall-runoff response in the New River (Hall et al., 2012; Peierls et al., 2012). This is in stark contrast with the Neuse River and its lagged response to precipitation events. Both the NewRE and NeuseRE often experience vertical stratification and seasonal bottom water hypoxia.

2.2. Spatial surveys

One survey was conducted in the NewRE (Sept. 8, 2015) and NeuseRE (Sept. 29, 2015) before Hurricane Joaquin passed the study

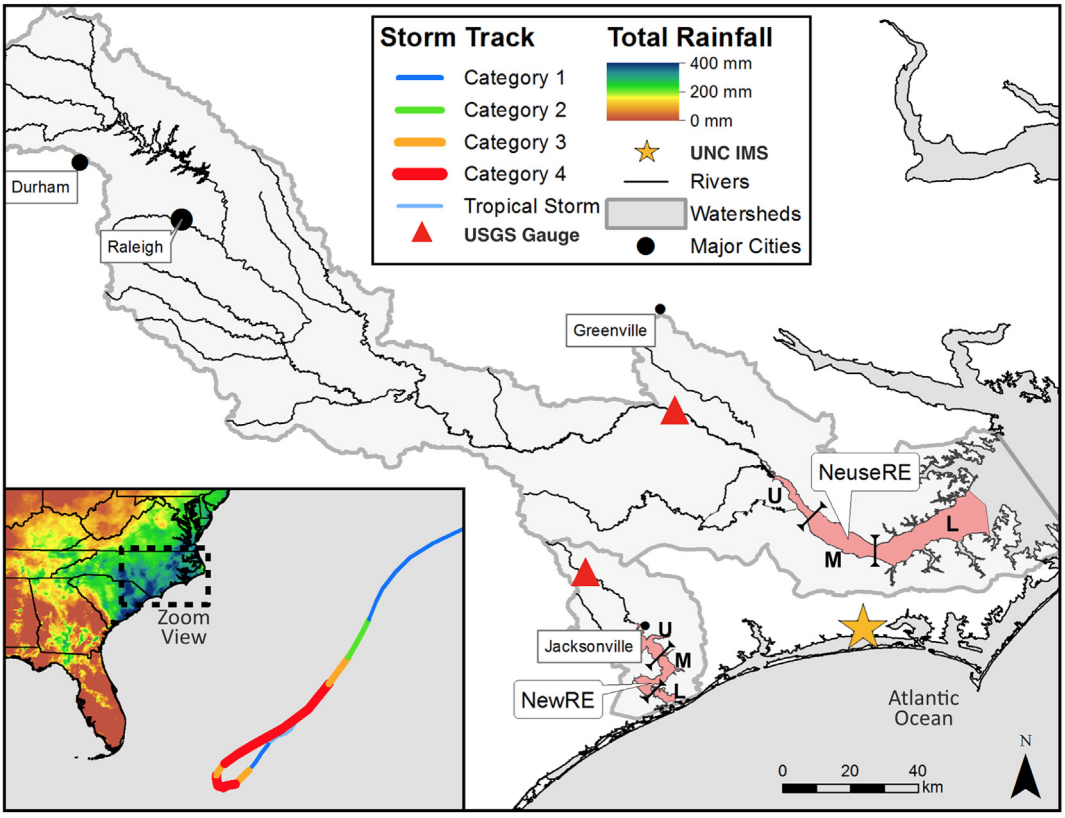

Fig. 1. Site map showing three-day rainfall totals (mm; October 1–3, 2015) and Hurricane Joaquin storm track (inset map), as well as the locations of the NewRE and NeuseRE within their respective watersheds. Upper (U), middle (M), and lower (L) estuarine segments are shown in pink. Rainfall averages were obtained from the PRISM database (http://www.prism.oregonstate.edu/), and the storm track was acquired from the National Hurricane Center (http://www.nhc.noaa.gov/gis/). (For interpretation of the references to colour in this figure legend, the reader is referred to the web version of this article.)

area, and is considered representative of "Pre-flood" conditions. Another survey was conducted on Oct. 7, 2015 in the NewRE, and on Oct. 12, 2015 in the NeuseRE, which we consider to be "flood" surveys because they coincide with peak discharge from both rivers. A final survey was conducted in each estuary after river discharge returned to pre-flood levels, on Oct. 29 and Nov. 4 in the NeuseRE and NewRE, respectively. Hurricane Joaquin passed well east (~900 km) of the study area as a category 3 or 4 storm, producing > 38 cm of rainfall over much of the study area, including most of the New and Neuse River watersheds (Fig. 1). In contrast to direct hurricane landfalls (Hurricane Irene, 2011), wind speeds over eastern NC remained relatively low during Joaquin, rarely exceeding 20 m s^{-1}. These surveys took place in conjunction with well-established water-quality monitoring programs, DCERP and ModMon, that were previously expanded to include high-resolution pCO_2 spatial surveys. Each survey consisted of a transect along the longitudinal axis of the estuary (Fig. 1), where a flow-through system was used to collect underway pCO_2 and auxiliary parameters at 0.5 hz, corresponding to an approximate spatial resolution of 10–20 m. Surveys began at a mid-morning time (~09:00 am) at the seaward extent of each estuary and proceeded up-estuary, finishing in the early afternoon. Detailed descriptions of the methods, including equipment calibration procedures are available (Crosswell et al., 2012; Van Dam et al., 2018).

2.3. Discrete samples

At 8 stations in the NewRE, and 12 in the NeuseRE, water was sampled in conjunction with water-quality monitoring programs ModMon and DCERP. At each station, approximately 2 L of water was collected using a diaphragm pump, at both surface and bottom depths (0.1 below surface and 0.5 m above bottom respectively). Samples were stored covered in a cooler, and processed upon return to the lab, following methods previously reported for analysis of dissolved organic carbon (DOC), total dissolved nitrogen (TDN), and Chlorophyll-a (Chl-a) (Peierls et al., 2012). Subsamples for dissolved inorganic carbon (DIC) were taken upon return to the lab, typically 4–6 h after bulk water samples were collected, and stored in unpreserved 20 mL scintillation vials with no headspace. DIC was then determined within 24 h using a Shimadzu TOC-5000A in inorganic carbon mode. A difference between DIC in preserved and unpreserved samples taken in this manner exists (regression standard error = 57.64 μmol kg^{-1}; Crosswell et al., 2012), but this difference is small relative to observed spatial and temporal variability in DIC. Therefore, we did not apply a correction to the DIC values in this study. At each station, a vertical profile of salinity (Sal), temperature (T), pH, DO, and Chl-a was conducted at a resolution of ~0.5 m using a YSI 6600 datasonde. Additional carbonate system parameters like Total Alkalinity (TA) and Revelle Factor (R) were calculated using CO2SYS (Lewis and Wallace, 1998), according to the carbonic acid dissociation constants of Millero (2010), and the NBS buffer scale. The use of carbonic acid dissociation constants from Millero (2010) may cause pCO_2 to be significantly overestimated, especially at low salinity (Dinauer and Mucci, 2017). However, in this study, estimates of TA and R were relatively robust to different dissociation constants. Directly measured pCO_2, DIC, T, and Sal were used as inputs in all cases.

2.4. CO_2 flux

Air-water CO_2 fluxes were determined by first assembling distance-weighted averages of pCO_2, T, and Sal for upper, middle, and lower estuarine segments (Fig. 1). Air-water CO_2 exchange was then calculated from pCO_2, Sal, and T by:

$$\text{flux} = k * K_o * \Delta pCO_2 \quad (1)$$

where ΔpCO_2 is the air-water pCO_2 gradient (μatm), and by convention, a positive ΔpCO_2 indicates CO_2 release to the atmosphere. K_o is the T- and Sal-dependent solubility coefficient for CO_2 (Weiss, 1974), and k is the gas transfer velocity (cm h^{-1}). The choice of different k parameterizations can yield widely diverging calculated CO_2 fluxes. We chose the parameterization of Jiang et al. (2008) because it is a moderate estimate of k that integrates data from both marine- and river-dominated estuaries, and is consistent with previous studies in the NewRE and NeuseRE (Crosswell et al., 2012; Crosswell et al., 2017; Van Dam et al., 2018). In all cases, daily average wind speeds were obtained from two autonomous vertical profilers deployed in the NewRE (Reynolds-Fleming et al., 2002), and from two meteorological stations (KEWN and KNKT) near the NeuseRE (Fig. 1). Due to obvious safety concerns, no measurements were made during the storm.

2.5. Thermal effects

The solubility of CO_2 varies inversely with T, causing pCO_2 to decrease by ~50% for every 16 °C decrease in T (Takahashi et al., 1993). This solubility effect acts in concert with mixing, atmospheric exchange, and biological consumption/production to alter pCO_2. We applied the formulas of Takahashi et al. (2002), which were used to assess the temperature effect on pCO_2, using a standard temperature effect ($\partial \ln pCO_2/\partial T$) of 0.0423 $°C^{-1}$. It is acknowledged that this temperature effect is not a constant, and in fact may fall below 0.03 $°C^{-1}$ in river-dominated estuaries (Jiang et al., 2008; Joesoef et al., 2015). However, the use of this constant temperature effect allows us to present an upper-bound for the temperature effect, and importantly, a conservative estimate for combined non-thermal drivers (biology, mixing, air-water exchange). In estimating thermal effects on variations in pCO_2, it is useful to assume some average value for pCO_2, and calculate the effect of known changes in temperature. To do this, average pCO_2 (for the entire study period) was normalized to the observed temperature at each sampling time, such that $pCO_2(T) = pCO_{2(avg)} * \exp[0.0423 * (T_{Obs} - T_{Avg})]$. $pCO_{2(avg)}$ was 1217 and 755 μatm in the NewRE and NeuseRE respectively, T_{Obs} is the observed temperature, and T_{avg} is the study-average temperature (23.5 and 22.8 °C in the NewRE and NeuseRE). $pCO_2(T)$ was calculated for each estuarine station, then averaged over each segment shown in Fig. 1. It should be noted that variations in $pCO_2(T)$, by this estimate, are only a function of changes in temperature, and are independent of variations in observed pCO_2. Next, measured pCO_2 ($pCO_{2(obs)}$) was normalized to T_{avg}, allowing us to calculate pCO_2(N-T), which represents the combined non-thermal effects on pCO_2, *after* the effect of temperature changes on solubility have been approximated: $pCO_2(N\text{-}T) = pCO_{2(obs)} * \exp[0.0423*(T_{obs} - T_{avg})]$. Finally, the average thermal and non-thermal effects on pCO_2 over the entire study period were then determined as the range (maximum – minimum) in $pCO_2(T)$ and pCO_2(N-T) respectively. It is important to note that $pCO_2(T)$ and pCO_2(N-T) calculated in this manner are *not* intended to represent two components of measured pCO_2, such that $pCO_2(T) + pCO_2(N\text{-}T) = pCO_{2(obs)}$. Instead, $pCO_2(T)$ and pCO_2(N-T) are independent estimates of the relative impact of thermal and non-thermal effects on variations in pCO_2.

2.6. Timescales of flushing and air-water exchange

Previous studies have shown that freshwater age (τ_{FW}), or flushing time, along with organic matter (OM) and nutrient supply, drive inter-annual variability in CO_2 fluxes (Laruelle et al., 2017), especially in poorly flushed lagoonal estuaries like the NewRE (Crosswell et al., 2017) and NeuseRE (Van Dam et al., 2018). Here, we calculate τ_{FW} using the date-specific freshwater replacement method of Alber and Sheldon (1999). Details of the adaptation of this method to the NewRE and NeuseRE can be found in Crosswell et al. (2017) and Van Dam et al. (2018). Similar to the concept of τ_{FW} is that of gas transfer residence time (τ_{GTV}), which is the amount of time required for dissolved gasses in a given parcel of water to come to equilibrium with the atmosphere, holding all other exchanges constant. For an ideal gas, τ_{GTV} is

proportional to the depth of the surface mixed layer (h) divided by the molecular diffusivity (D/z) (Broecker and Peng, 1974). Because CO_2 exchanges not only with the atmosphere, but also with the carbonate buffering system, τ_{GTV} for CO_2 increases with the size of the DIC pool and 1/pH, and can be approximated by the following equation (Ito et al., 2004; Jones et al., 2014):

$$\tau_{GTV} = \frac{h}{k*R} * \frac{DIC}{pCO_2 * K_o} \quad (2)$$

where k is the gas transfer velocity, R is the Revelle factor (calculated in CO2sys from pCO_2, DIC, T, and Sal), and K_o is the CO_2 solubility. For surveys where vertical stratification was evident in a given segment ($Sal_{surface} - Sal_{bottom} > 3$; n = 3 in the NewRE, n = 5 in NeuseRE), h was approximated as half of the total water depth; h was set to the total water depth when waters were vertically mixed.

3. Results

3.1. Pre-flood surveys (Sept 8-Sept 30, 2015)

Prior to the arrival of hurricane Joaquin, discharge from the New and Neuse River fluctuated around median values for the season (Fig. 2a,b), and both estuaries were weakly stratified with hypoxic to anoxic bottom waters (Table 1). Consistent with typical Fall conditions and relatively high T (26–29 °C), PPR and Chl-a were elevated in the upper regions of both estuaries. As reported previously for the NeuseRE under moderate-flow conditions, pCO_2 was spatially variable in the lower estuary, with regions above and below equilibrium with the atmosphere (Fig. 3) (Crosswell et al., 2012; Van Dam et al., 2018). Due to the high spatial variability in pCO_2 in the NeuseRE, and high salinity in the NewRE, average pre-storm CO_2 fluxes were low, at < 20 mmol C m^{-2} d^{-1} in both estuaries (Table 2).

3.2. Event characterization

Hurricane Joaquin reached tropical storm designation on Sept 29, 2015 and peaked at category 4 status just north of the Bahamas on October 3 (Berg, 2016). While the hurricane passed well east (~900 km) of the study area, moisture associated with the storm interacted with a stalled low-pressure system that lingered over the southeastern US, contributing to significant rainfall and historic flooding in South and North Carolina. Total rainfall during this event was > 38 cm over much of the study area, including most of the New and Neuse River watersheds (Fig. 1). This precipitation drove peak river discharges of 53 and 278 $m^3 s^{-1}$ in the New (Oct 4, 2015) and Neuse (Oct 7, 2015) respectively. Wind speeds over eastern NC were only moderately impacted by hurricane Joaquin; daily averages were always < 10 m s^{-1}, and gusts rarely exceeded 20 m s^{-1}. This is in contrast with previous hurricanes to directly impact the study are, like Irene, when sustained winds were 30–40 m s^{-1}.

3.3. Flood surveys (Sept 30-Oct 13, 2015)

Strong NE winds have been shown to disrupt vertical stratification in the NeuseRE (Luettich et al., 2000), and winds above 7 m s^{-1} can drive sediment re-suspension in the NewRE (Brown et al., 2014; A. Whipple, personal communication) Conditions such as these persisted from Oct 3 to 7, which thoroughly mixed the middle NewRE, although stratification persisted throughout the storm in the upper estuary (Fig. 4a). Continuous vertical profile data were not collected in the NeuseRE, but wind speeds of up to 10 m s^{-1} during the storm (Fig. 2a) likely drove some degree of vertical mixing (Luettich et al., 2000). Nevertheless, the Oct 12 survey in the NeuseRE showed strong stratification, suggesting that wind-driven vertical mixing was not sufficient to completely aerate bottom waters. This is in stark contrast to the impact of Hurricane Irene on the NeuseRE, where inferred sediment re-

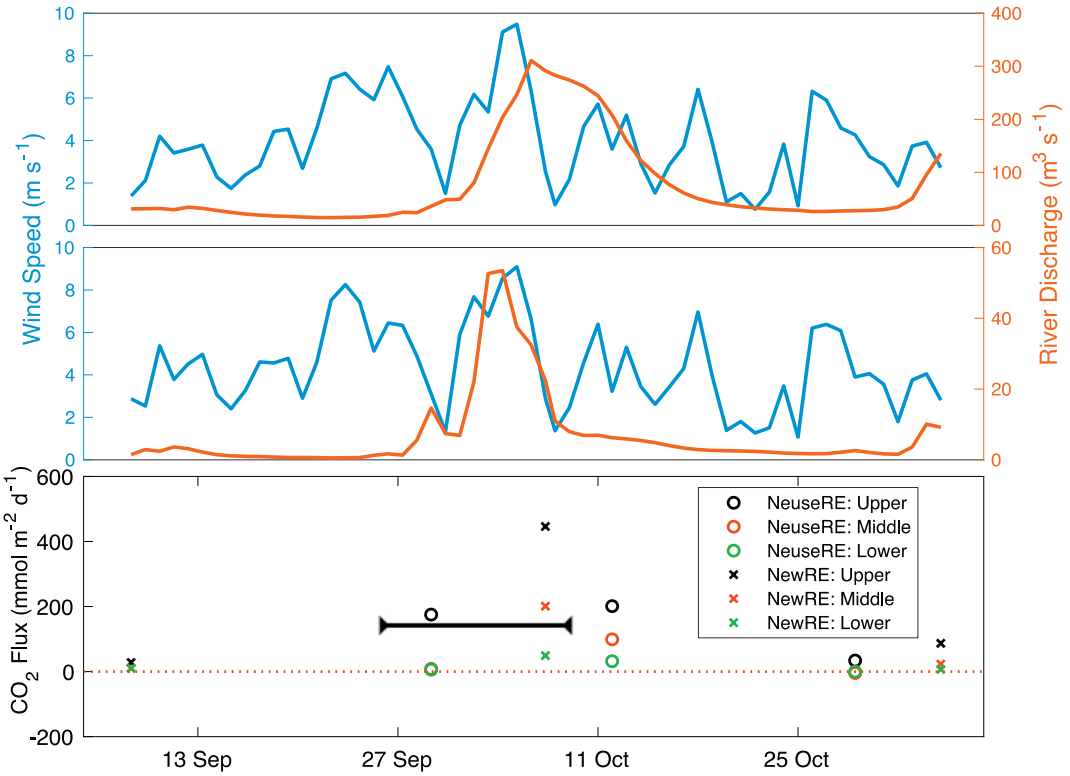

Fig. 2. Time-series of river discharge ($m^3 s^{-1}$) and wind speed (m s^{-1}) in the NeuseRE (a) and NewRE (b). Time-series of sectional-average CO_2 fluxes for both estuaries (c); the horizontal line represents net air-water equilibrium with respect to CO_2. The period of maximum storm impact is indicated by the black arrow on the date axis.

Table 1
River end-member DOC/DIC/DIN values for each survey date, along with the expected concentration derived from the best-fit equations shown in Fig. 4.

		Measured				Expected (long-term average)			% difference		
	Survey date	Discharge (m3/s)	DOC (μM)	DIC (μM)	TDN (μg L^{-1})	DOC (μM)	DIC (μM)	TDN (μg L^{-1})	DOC (μM)	DIC (μM)	TDN (μg L^{-1})
New river	9/8/15	1.1	929	1615	127	637	1871	156	46	−14	−19
	10/7/15	37.5	2174	507	115	1560	389	128	39	30	−10
	11/4/15	7.1	1314	902	133	1022	818	140	29	10	−5
Neuse river	9/29/15	36.1	559	825	53	541	532	62	3	55	−15
	10/12/15	209.2	894	325	61	723	337	77	24	−3	−21
	10/29/15	28.0	526	708	81	519	569	60	1	25	35

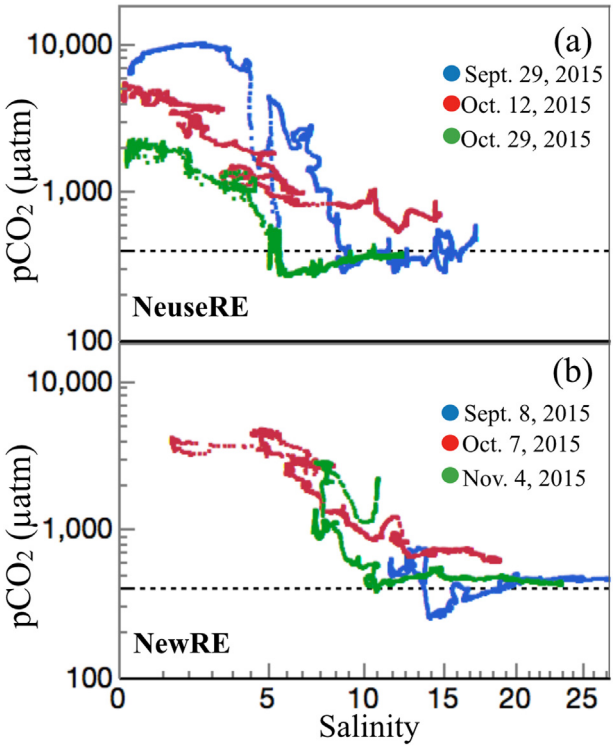

Fig. 3. Scatter plots of salinity vs pCO_2 (μatm) in the NeuseRE (a) and NewRE (b), for pre-flood (blue), flood (red), and post-flood (green) surveys. The horizontal black dotted line represents approximate equilibrium with the atmosphere (pCO_2 = 400 μatm). (For interpretation of the references to colour in this figure legend, the reader is referred to the web version of this article.)

suspension and water column de-stratification supported approximately 40% of during-storm CO_2 fluxes (Crosswell et al., 2014).

High river discharge was associated with increased DOC and decreased DIC concentrations in both rivers, consistent with a logarithmic relationship between DOC (positive slope) or DIC (negative slope) with discharge (Fig. 5). No clear relationship between TDN and discharge was observed. The concentration of DOC during the storm exceeded the value predicted by the relationship between discharge and concentration in both estuaries (Table 1), suggesting the input of additional terrestrial organic matter. DIC during the storm was greater than a log-linear relationship between discharge and concentration would predict (Fig. 5), by a factor of ~30% in the New River. However, DIC did not depart significantly from the long-term relationship between discharge and concentration in the Neuse River. Consistent with elevated DOC loading, and reduced PPR (Table 3), ΔpCO_2 rose rapidly to a maximum of 4293 and 3302 μatm in the NeuseRE and NewRE respectively. Increases in pCO_2 were strongly associated with decreased T, DO, Sal, and pH, which fell steadily in both estuaries until reaching a minimum on Oct 12 (NeuseRE) and Oct 7 (NewRE) (Table 3). DO fell to 65 and 57% in the upper NewRE and NeuseRE respectively, suggesting that much of the pCO_2 increase was generated through the respiration of terrestrial organic matter. Average CO_2 fluxes for the during-storm period were between 4 and 16 times greater than during the pre-storm period, 265 and 62 mmol C m^{-2} d^{-1} in the NewRE and NeuseRE respectively (Table 2).

3.4. Post-flood surveys (Oct 13-Nov 4, 2015)

River discharge began to decrease in the week following the storm (Fig. 2a,b), but historic rainfall in the upper reaches of the watershed (Fig. 1) maintained levels well above base-flow. DOC inputs from the New River remained high after the storm, compared with values predicted by the log-linear relationship with discharge (Fig. 5b), while DOC in the Neuse River returned to predicted concentrations by the 29 Oct survey (Table 1). Both estuaries were moderately to strongly

Table 2
Average ΔpCO_2 (μatm) and CO_2 flux (mmol C m^{-2} d^{-1}) for each survey period before, during, and after flooding. Total column represents the sum of sectional averages, weighted by the respective surface area of each segment.

		Upper		Middle		Lower		Total	
		ΔpCO_2	CO_2 Flux	ΔpCO_2	CO_2 Flux	ΔpCO_2	CO_2 Flux	ΔpCO_2	CO_2 Flux
NeuseRE	9/29/15 Pre-flood	2790	175	113	8.3	81	5.7	258	17
	10/12/15 Flood	4293	201	1671	99	562	32	1109	62
	10/29/15 Post-flood	628	34	−59	−4.2	0.25	0.017	22	0.9
NewRE	9/8/15 Pre-flood	617	28	252	11	233	9.6	379	17
	10/7/15 Flood	3302	446	1530	201	389	49	1982	265
	11/4/15 Post-flood	1550	87	409	23	132	6.9	772	43

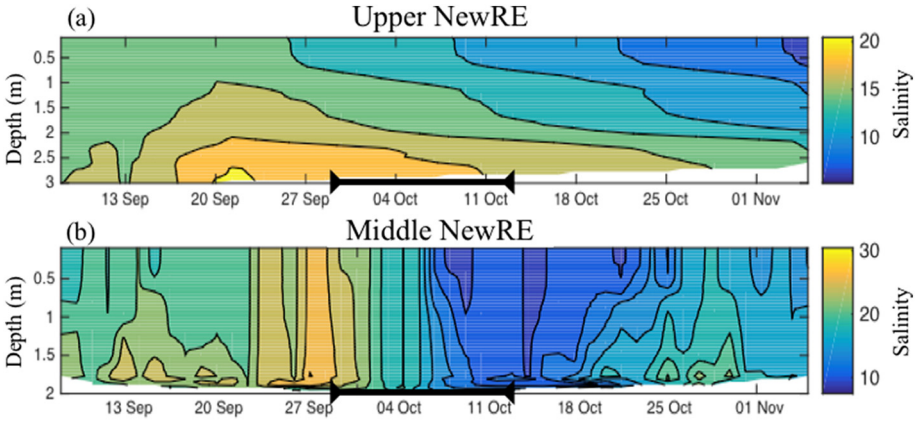

Fig. 4. Time-series contour plots showing vertical salinity distributions in the upper NewRE (a), and middle NewRE (b). The period of maximum storm impact is indicated by the black arrow on the date axis. Data collected by Autonomous Vertical Profiler (AVP) buoys at two stations in the NewRE.

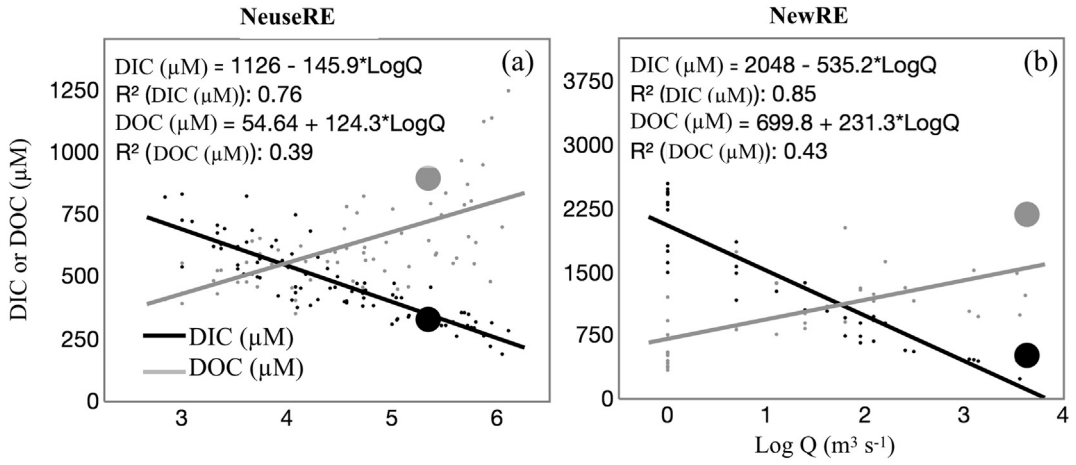

Fig. 5. Scatter plots of river discharge (Q, $m^3 s^{-1}$) against DIC (µM) and DOC (µM) for the Neuse RE (a) and NewRE (b), where the sampling point closest in time to peak storm flow is emphasized as the enlarged dot. Linear regression and correlation coefficients (R^2) are shown for the relationship between log Q and solute concentration.

stratified during the post-flood survey, and bottom waters were hypoxic or sub-oxic (Table 3). Despite moderate decreases in ΔpCO_2 accompanied by elevated DO and Chl-a in the upper NewRE, low rates of PPR kept ΔpCO_2 above 0, between 132 and 1550 µatm in the lower and upper segments, respectively (Fig. 2). In the NeuseRE, however, ΔpCO_2 fell to 0 and − 59 in lower and middle segments by the time of the post-storm survey on October 29. This ΔpCO_2 decrease was accompanied by elevated Chl-a, DO, and PPR (Table 3). Despite net CO_2 uptake in the large lower segments, high ΔpCO_2 in the upper estuary (628 µatm) maintained small but positive CO_2 fluxes in the NeuseRE as a whole during the post-flood period (Fig. 2a). Average CO_2 fluxes during this period reflect combined increases in DOC and DIC loads, along with elevated phytoplankton biomass. Hence, post-storm CO_2 fluxes were midway between pre- and during-flood values, at 43 and 0.9 mmol C m^{-2} d^{-1} in the NewRE and NeuseRE respectively (Table 2).

3.5. *Timescales of flushing and air-water exchange*

Before the storm, cumulative τ_{FW} was 136 and 90 days in the NeuseRE and NewRE respectively, above the annual average (58 and 46 days), while τ_{GTV} was 6.5 and 6.8 days (Fig. 6). This is well below the approximately 1-year mean τ_{GTV} typically reported for the global ocean, but much closer to the week- or month-long time scale of many coastal and equatorial regions (Jones et al., 2014). It is unclear whether our estimates of τ_{GTV} are representative of other estuaries, either globally or regionally. As pCO_2 rose during the flood surveys, τ_{GTV} correspondingly fell by around 60% to 2.0 and 2.6 days in the NeuseRE and NewRE respectively. At the same time, elevated river discharge caused average τ_{FW} in the NewRE to rapidly fall to 9 days. Total τ_{FW} for the NeuseRE only fell to 128 days, apparently due to the slow response time of the large lower segment of this estuary. τ_{FW} in the relatively small upper and middle segments of the NeuseRE were 1.7 and 8.4 days, respectively, during the storm survey. After the study period, a series of winter storms inundated the watershed in the months following Joaquin, decreasing τ_{FW} in the lower NeuseRE to a minimum of 19.8 days on 20 January 2016 (Van Dam et al., 2018).

In both estuaries, τ_{FW} and τ_{GTV} decreased during Joaquin, indicating that water spent less time in the estuary, while at the same time, CO_2 was vented more rapidly to the atmosphere. This was most prominent in the NewRE, where τ_{FW} was approximately 20 times greater than τ_{GTV}. Both τ_{FW} and τ_{GTV} were very low in the upper NeuseRE, but τ_{FW} in the lower segment did not change significantly during the storm, due to a large lag-time between water leaving the head of the estuary and reaching this segment. We can summarize by inferring that both τ_{FW} and τ_{GTV} responded similarly to the elevated discharge during Joaquin across the entire NewRE. In the NeuseRE, however, there was a longitudinal gradient. The upper estuary was sensitive to changes in both τ_{FW} and τ_{GTV}, while the lower segment only responded to changes in τ_{FW}.

Table 3
Segment- and volume-weighted averages for select parameters before, during, and after storm.

	Date	Depth	T			Sal			DO (mg/L)			pH			DOC (μM)			DIN (μM)			Total Chlorophyll-a (μg L^{-1})			PPR (mg C m-3 h-1)		
			U	M	L	U	M	L	U	M	L	U	M	L	U	M	L	U	M	L	U	M	L	U	M	L
NeuseRE	9/29/15	Surf.	24	25	24	6	11	15	6.6	8.8	8.7	7.4	7.9	7.9	905	540	450	8	1	1	91.3	14.9	21.1	49	89	107
	Pre-Flood	Bot.	24	24	24	9	12	17	4.2	6.9	6.1	7.0	7.5	7.5	630	517	426	11	2	7	9.4	9.5	5.7			
	10/12/15	Surf.	20	20	21	1	4	11	5.5	7.4	7.7	6.8	7.2	7.5	970	1033	644	26	21	6	0.4	6.3	17.3	2	28	70
	Flood	Bot.	22	22	22	10	11	14	1.9	3.8	6.1	6.5	6.8	7.3	642	560	557	25	18	8	2.5	3.1	7.4			
	10/29/15	Surf.	20	20	19	4	7	11	9.0	9.8	9.0	7.5	7.8	7.7	793	807	681	24	2	1	25.1	35.6	23.2	134	166	104
	Post-Flood	Bot.	20	19	19	6	8	14	4.9	6.8	7.4	7.1	7.4	7.5	782	765	572	29	2	2	7.8	18.7	10.4			
NewRE	9/8/15	Surf.	28	28	28	13	18	28	7.3	7.5	6.3	7.8	7.9	7.8	684	534	284	1	2	4	81.9	14.0	8.8	96	51	78
	Pre-Flood	Bot.	28	28	27	16	23	31	3.8	4.1	6.1	7.4	7.5	7.9	595	429	229	4	13	3	15.7	5.4	8.6			
	10/7/15	Surf.	21	21	21	5	10	18	6.1	7.5	7.3	7.0	7.3	7.5	1417	895	585	18	20	19	4.0	8.1	6.1	13	19	16
	Flood	Bot.	22	22	21	12	18	20	5.3	5.8	6.9	6.9	7.3	7.6	711	581	520	22	24	17	2.8	1.8	5.6			
	11/4/15	Surf.	19	20	20	9	13	21	7.2	7.8	7.2	7.3	7.6	7.6	941	848	542	18	17	15	54.9	9.8	3.8	67	21	12
	Post-Flood	Bot.	20	20	20	13	18	25	3.7	6.4	6.9	7.1	7.5	7.6	796	636	427	25	20	12	3.6	1.2	3.4			

4. Discussion

4.1. Role of flooding in the context of annual CO_2 fluxes

Annual CO_2 emissions for the 2015 water-year (27 Oct 2014–26 Oct 2015) were 15.7 and 7.7 mmol C m^{-2} d^{-1} (Van Dam et al., 2018), corresponding to a total annual flux of 4.5×10^8 and 9.9×10^8 mol C in the NewRE and NeuseRE, respectively. Average CO_2 fluxes during the storm surveys were 265 and 62 mmol m^{-2} d^{-1} in the NewRE and NeuseRE (Table 1), corresponding to a total flux of 3.0×10^8 and 3.1×10^8 mol C, if daily fluxes are scaled up to the 14 day 'storm' period. Hence, CO_2 fluxes during Joaquin were responsible for approximately 44% of the total annual flux in the NewRE, and 31% in the NeuseRE. Crosswell et al. (2014) determined that the combined effects of high winds and storm surge during Hurricane Irene drove CO_2 fluxes of 4080 mmol C m^{-2} d^{-1}, approximately 9 times higher than the maximum observed value of 446 mmol C m^{-2} d^{-1} during this study (Fig. 2). Wind-dominated events in other estuaries were associated with CO_2 fluxes well below those during Irene (Fig. 7). Flooding events had variable impacts on air-water CO_2 exchange, from a minimum of 51.5 mmol C m^{-2} d^{-1} in a small New England estuary, to a maximum of 669 mmol C m^{-2} d^{-1} for the Mississippi River plume, with CO_2 fluxes determined in the present study lying between these extremes. Both the NewRE and NeuseRE have the potential to be net sinks for atmospheric CO_2 during relatively dry years, and are otherwise small CO_2 sources (Crosswell et al., 2012, 2014, 2017; Van Dam et al., 2018). Therefore, it is clear that storm events such as Joaquin must be accounted for when estuarine CO_2 fluxes are incorporated into annual ecosystem C budgets, or broader, regionally or globally scaled budgets.

4.2. Drivers of pCO_2: thermal effects

Before the storm, pCO_2(T) was well above pCO_2(N-T) in the NewRE and all but the upper NeuseRE. As cooler floodwaters entered both estuaries, pCO_2(T) decreased slightly, but pCO_2(N-T) increased by a factor of 2-8× (Fig. 8b-g). Hence, the rapid increase in pCO_2 observed during the storm was driven by inputs of CO_2 from mixing and net respiration, which far outweighed the thermal effect, acting to decrease pCO_2. Following the storm, pCO_2(N-T) began to fall as PPR increased (Table 3) and DOC loads decreased (Table 1), while pCO_2(T) remained relatively low. Over the entire study period, however, pCO_2 closely tracked pCO_2(N-T), suggesting that non-thermal effects like net ecosystem metabolism and mixing drove temporal variations in pCO_2. The ratio of thermal to non-thermal effects (T/N-T = pCO_2(T)/pCO_2(N-T)) was below 0.3 in all estuarine segments except the lower NewRE (T/N-T = 0.76). In this portion of the lower NewRE, PPR and Chl-a are generally low (Table 3), and the estuary is strongly influenced by tidal exchange with the ocean.

While non-thermal drivers of pCO_2 (net biological and mixing effects) were dominant during this flooding event, solubility-related thermal effects were non-negligible. We estimate that if T had remained at pre-flood values throughout the storm, average pCO_2 for the flood survey would have increased from 2431 and 1563 μatm to 3341 and 1964 μatm in the NewRE and NeuseRE respectively (holding the biological effect of decreased T constant). Hence, cooler temperatures during the flood had the counterintuitive effect of reducing pCO_2 by between 27 and 38%. Similarly, the return of warmer, saltier water was responsible for an approximate doubling of pCO_2 after a large flood in a subtropical Australian estuary (Ruiz-Halpern et al., 2015), although this effect was limited to downstream reaches closest to the ocean. On the contrary, thermal effects were deemed insignificant during Hurricane Irene (Crosswell et al., 2014), highlighting an important distinction between wind- and flood-driven events. While relatively stable temperatures typical of a wind-dominated event may allow biological and physical factors to drive variations in pCO_2, temperature change during flooding may conceal or amplify these non-thermal pCO_2 variations. In

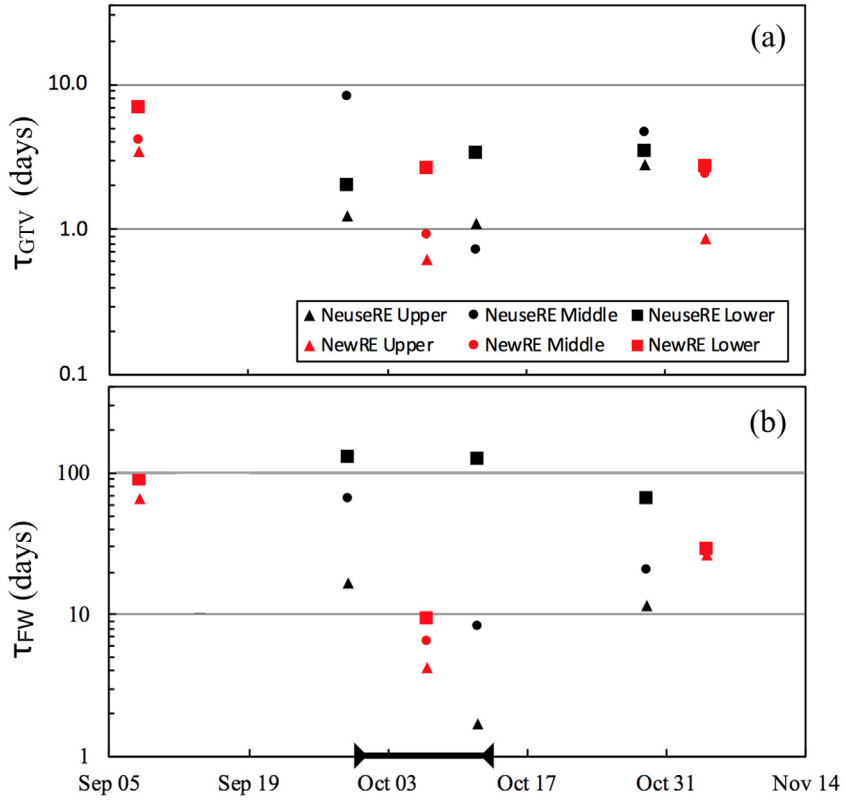

Fig. 6. Time-series plots of τ_{GTV} (a) and τ_{FW} (b) for the NewRE and NeuseRE. The period of maximum storm impact is indicated by the black arrow on the date axis.

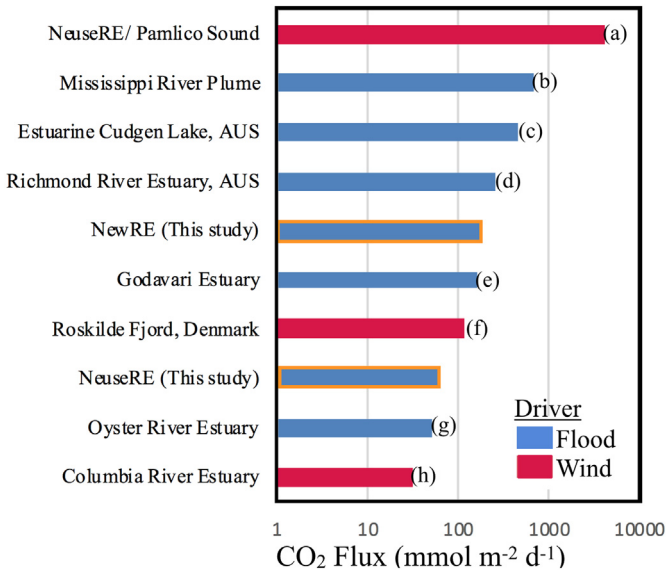

Fig. 7. Horizontal bar chart of storm-driven CO_2 fluxes (mmol m^{-2} d^{-1}) derived from the literature, separated by whether the dominant driver was flooding (blue) or wind-induced mixing (red). The golden highlighted bars show the results of this study. References are as follows: a) Crosswell et al., 2014; b) Bianchi et al., 2013; c) Jeffrey et al., 2016; d) Ruiz-Halpern et al., 2015; e) Sarma et al., 2011; f) Mørk et al., 2016; g) Hunt et al., 2011; h) Evans et al., 2012. (For interpretation of the references to colour in this figure legend, the reader is referred to the web version of this article.)

the present study, cool fresh water extended across the length of both estuaries (Table 3), effectively 'trapping' CO_2 in the water by increasing its solubility and limiting its loss to the atmosphere. Hence, the net result of this thermal effect was that more of the CO_2 generated within the estuary (or brought in from the river) was transported laterally to the coastal ocean, rather than being lost to the atmosphere via air-water exchange. This lateral export of CO_2 may have been significant to the annual C budget of these estuaries, but a precise quantification of this flux is beyond the scope of this study.

4.3. *Drivers of pCO_2: non-thermal effects*

4.3.1. *Variability in end-member TA and DIC*

Respiratory inputs often drive CO_2 emissions during storms, but this CO_2 may be produced within the estuary (Crosswell et al., 2014; Ruiz-Halpern et al., 2015) or in the watershed, and be transported in by rivers (Hunt et al., 2011, 2014; Van Dam et al., 2018). DOC loads from both the New and Neuse Rivers increased during the storm, beyond levels that would be expected for the respective discharge conditions (Table 1), providing ample organic material to support heterotrophic processes in the estuary. However, inputs of DIC and TA from rivers may also vary with discharge, and the ratio of DIC:TA significantly impacts carbonate system buffering (Joesoef et al., 2017). Hence, these altered DIC and TA loads may also affect the fate of CO_2 in the estuary. Trends in TA across both the NewRE and NeuseRE were dominated by mixing between marine water high in TA, and river water relatively depleted in TA (Fig. 9b). Before the storm, mixing plots show river water (Sal = 0, TA~900 μM) mixing conservatively with the saltwater end-members in Pamlico Sound (Sal~20, TA~1500 μM) and Onslow Bay (Sal~35, TA~2100 μM). During the storm surveys, the saltwater end members remained constant, while both riverine end-member TA values fell dramatically, to approximately 270 μM. Following the storm, riverine TA recovered to nearly pre-storm values, while rainwater diluted both the Pamlico Sound (Sal = 20, TA~1000 μM) and Onslow Bay (Sal = 30, TA~1500 μM) end-members. Accounting for these shifting end members, conservative mixing appeared to govern TA distributions in both the NewRE and NeuseRE throughout the study. A variety of redox and geochemical reactions can contribute to non-conservative behavior in the TA vs salinity relationship (Cai et al.,

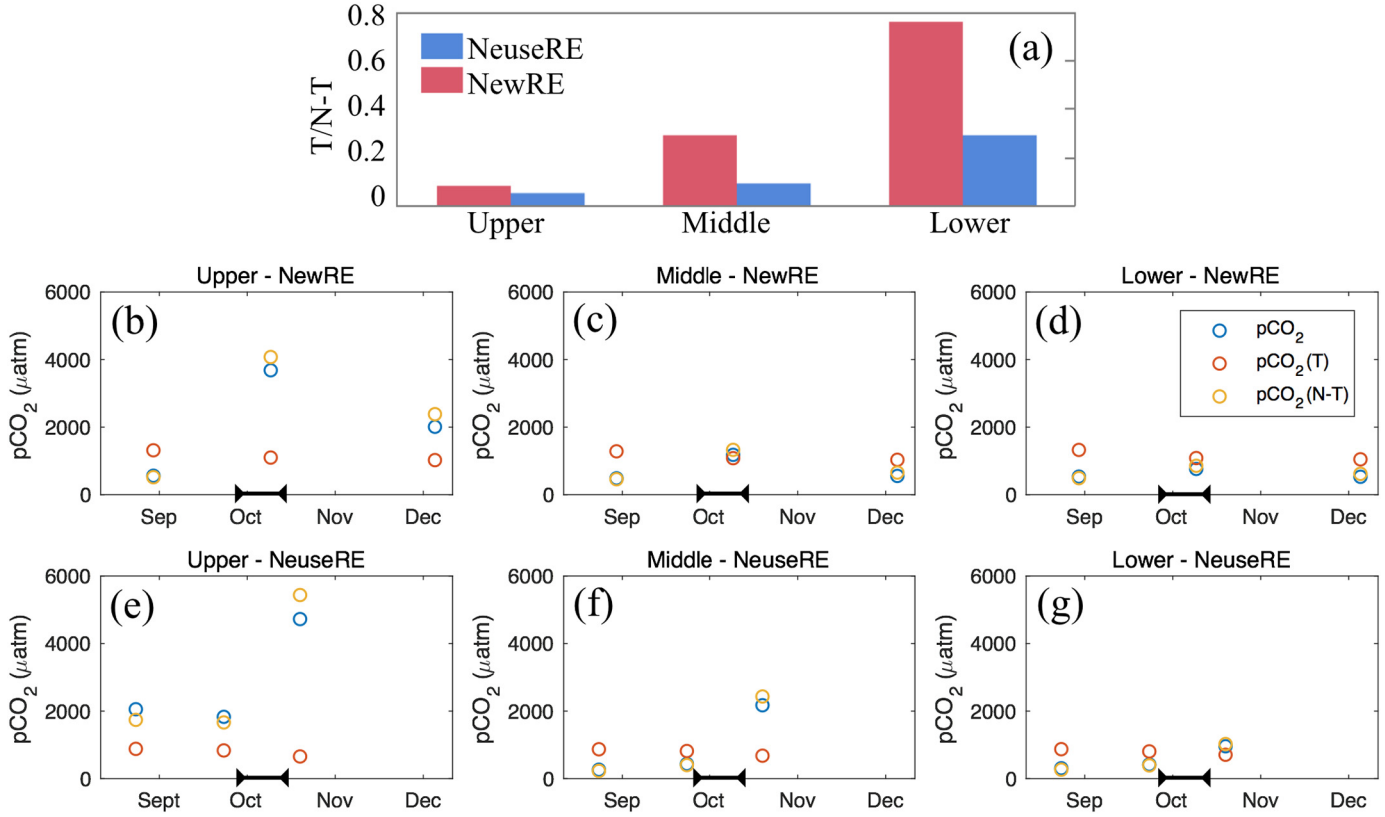

Fig. 8. Bar graph of sectional mean T/N-T for each estuary (a). Time series plots of pCO_2, pCO_2(T), and pCO_2(N-T) for the NewRE (b-d) and NeuseRE (e-g). Arrows indicate approximate duration of storm impact. In figures b-g, pCO_2 is not equal to the sum of pCO_2(T) and pCO_2(N-T). As discussed earlier, pCO_2(T) and pCO_2(N-T) are not intended to represent two components of measured pCO_2, but instead, are independent estimates of the relative impact of thermal and non-thermal effects on variations in pCO_2.

2017), but these TA sinks/sources must have been in balance, or small relative to mixing.

While trends in TA through Joaquin were similar between both estuaries studied, a combination of factors caused the ratio of TA:DIC to vary with discharge, with important implications for acid-base buffering. Previous studies have identified variations in TA:DIC as an important driver of estuarine DIC dynamics (Joesoef et al., 2017; Li et al., 2017). As discussed in Hu and Cai (2013), estuaries where TA:DIC ratio falls below 1 may exhibit larger pCO_2 variations than those where TA:DIC remains above 1 across the system (Yao and Hu, 2017). In both the Neuse and New rivers, this TA:DIC ratio is most often below 1, as reflected in the low-salinity values in Fig. 9b. TA:DIC fell significantly during the storm in the upper NeuseRE, but by a lesser amount in the NewRE. The effect of changing TA:DIC on buffering can be represented with a commonly-used buffer factor, the Revelle factor (R), which is defined as $\partial\ln(pCO_2)/\partial\ln(DIC)$. R varied around 16 as an estuary-wide average, but a slight increasing trend (insignificant, p-value > 0.05) in both estuaries can be seen (Fig. 9a). Spatial trends, however, were more complex. Before the storm, R was ~15 in the upper regions of both estuaries, but low TA flood waters caused R to fall to 5.2 and 2.5 in the upper NewRE and NeuseRE respectively (Fig. 9a,b). It is likely that precipitation served to dilute TA of incoming river water, while DIC remained relatively high (perhaps due to respiratory inputs), effectively decreasing the TA:DIC ratio and thus R. Because R quantifies the sensitivity of pCO_2 to changes in DIC, we can estimate that, for a given respiratory addition of DIC, the subsequent increase in pCO_2 would have been ~5× larger in the lower estuary than in upper reaches.

Many estuaries exhibit a minimum buffer zone (MBZ), where R is locally maximized, and pCO_2 is most sensitive to DIC inputs (Hu and Cai, 2013). Van Dam et al., 2018 showed that under normal conditions the MBZ in the NewRE and NeuseRE occurred at salinity ranges of 10–15 and 4–8, respectively. Here, we show that the MBZ occurred in the same respective salinity ranges during floods, even though the entire gradient was shifted towards the ocean. Drawdowns in pCO_2 associated with the MBZ occurred in the lower regions of both estuaries; however, this region constitutes a large fraction (65%) of the total surface area of the NeuseRE, but a relatively small fraction of the NewRE (16%). Therefore, these pCO_2 reductions had a large influence in the NeuseRE, driving low CO_2 fluxes as a system-wide average, as opposed to the NewRE, where CO_2 drawdown in the lower estuary could not counteract high CO_2 flux in the upper estuary to the same extent as in the NeuseRE (Table 2). A similar mechanism was invoked to explain large storm-driven pCO_2 variations in the Columbia River estuary. There, extremely high values of R (~30) interacted with high wind speed to drive rapid air-water equilibration of CO_2 (Evans et al., 2012).

5. Conclusions

5.1. *Key drivers of pCO_2 and CO_2 fluxes during flooding*

Prior studies have demonstrated highly variable impacts of storms on CO_2 emissions from estuaries, ranging from CO_2 uptake (Evans et al., 2012) to significant CO_2 degassing (Sarma et al., 2011; Crosswell et al., 2014; Hunt et al., 2014; Mørk et al., 2016), with the sign and magnitude of CO_2 flux varying with storm characteristics and estuarine morphology. In this study, we expand on these studies by investigating the effect of a large flooding event on air-water CO_2 exchange in two adjacent, but markedly different, estuaries. Despite relatively low wind speed, CO_2 emissions during this ~14-day flood period were high, accounting for 31% to 44% of the total annual CO_2 flux in the NeuseRE and NewRE, respectively. Average CO_2 fluxes during Joaquin were

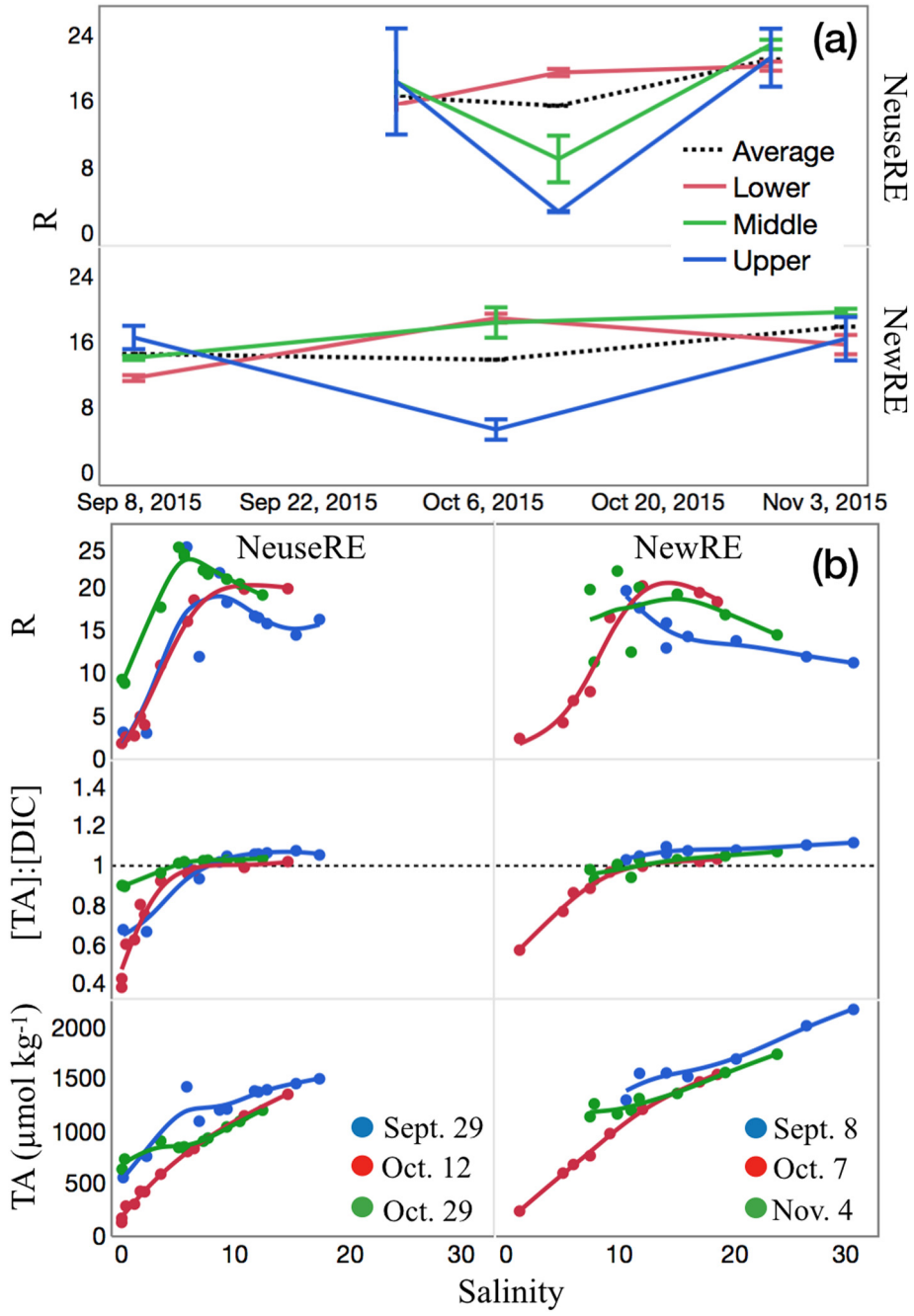

Fig. 9. Time series of sectional-mean Revelle factor for both estuaries (a). Mixing plots showing TA, TA:DIC, and R against salinity for pre-flood, flood, and post-flood samples (b).

within the range of other literature values for both wind-driven and flood events.

Massive inputs of low-alkalinity fresh water to the expansive lower NeuseRE, combined with a post-storm phytoplankton bloom, resulting in a rapidly draw-down of pCO_2. This CO_2 uptake counteracted relatively high CO_2 emissions in the upper NeuseRE, which was likely sustained by a combination of autochthonous and allochthonous CO_2. On the other hand, respiration of terrestrial organic matter combined with riverine C inputs drove large CO_2 emissions in the relatively large upper NewRE, which were not mitigated by a similar down-estuary bloom. While non-thermal drivers like biology, mixing and air-water exchange dominated variations in pCO_2 in the present study, the effect of decreasing temperature on increasing solubility was non-negligible. We estimate that a 5 °C drop in temperature during the storm drove pCO_2 reductions of ~30% in both estuaries, likely resulting in an increased export of DIC to the coastal ocean. The results of this study demonstrate that flooding events can contribute significantly to annual estuarine carbon budgets, and that sufficient spatial and temporal coverage during storms is necessary for estuarine CO_2 fluxes to be reliably assessed over annual time scales.

Acknowledgments

We appreciate the assistance of J. Braddy, H. Walker, B. Abare, K. Rossignol, R. Sloup and all individuals at VIMS and UNC-IMS who provided support in the field and lab. We thank the many collaborators and technical advisors within the Strategic Environmental Research and Developmental Program - Defense Coastal/Estuarine Research Program

(SERDP-DCERP) who have provided insightful comments, data and general guidance. We are also thankful to S. Cohen of NAVFAC and the Camp Lejeune Environmental Management Division staff. Raw data used in this study are provided as a compressed file in the supporting information; more detailed inquiries may be directed towards the corresponding author. Data for the NewRE are also available online at the following repository maintained by RTI International (https://dcerp.rti.org/login.aspx?ReturnUrl=%2fMARDISHome.aspx). This research was funded by SERDP-DCERP Project Number: RC-2245, The North Carolina Department of Environmental Quality (ModMon Program), the Lower Neuse Basin Association, NC Sea Grant and the UNC Water Resources Research Institute.

References

Alber, M., Sheldon, J.E., 1999. Use of a date-specific method to examine variability in the flushing times of Georgia estuaries. Estuar. Coast. Shelf Sci. 49 (4), 469–482. https://doi.org/10.1006/ecss.1999.0515.

Bauer, J.E., Cai, W.-J., Raymond, P.A., et al., 2013. The changing carbon cycle of the coastal ocean. Nature 504 (7478), 61–70. https://doi.org/10.1038/nature12857.

Berg, R.J., 2016. Tropical Cyclone Report: Hurricane Joaquin (2015). (National Hurricane Center).

Bianchi, T.S., Garcia-Tigreros, F., Yvon-Lewis, S.A., et al., 2013. Enhanced transfer of terrestrially derived carbon to the atmosphere in a flooding event. Geophys. Res. Lett. 40 (1), 116–122. https://doi.org/10.1029/2012GL054145.

Boyer, J.N., Christian, R.R., Stanley, D.W., 1993. Patterns of phytoplankton primary productivity in the Neuse River estuary, North Carolina, USA. Mar. Ecol. Prog. Ser. 97, 287–297.

Broecker, W.S., Peng, T.-H., 1974. Gas exchange rates between air and sea. Tellus 26 (1–2), 21–35. https://doi.org/10.1111/j.2153-3490.1974.tb01948.x.

Brown, M.M., Mulligan, R.P., Miller, R.L., 2014. Modeling the transport of freshwater and dissolved organic carbon in the Neuse River estuary, NC, USA following Hurricane Irene (2011). Estuar. Coast. Shelf Sci. 139, 148–158. https://doi.org/10.1016/j.ecss.2014.01.005.

Cai, W.-J., 2011. Estuarine and coastal ocean carbon paradox: CO_2 sinks or sites of terrestrial carbon incineration? Annu. Rev. Mar. Sci. 3 (1), 123–145. https://doi.org/10.1146/annurev-marine-120709-142723.

Cai, W.-J., Huang, W.-J., Luther, G.W., et al., 2017. Redox reactions and weak buffering capacity lead to acidification in the Chesapeake Bay. Nat. Commun. 8 (1), 369. https://doi.org/10.1038/s41467-017-00417-7.

Chen, C.-T.A., Borges, A.V., 2009. Reconciling opposing views on carbon cycling in the coastal ocean: Continental shelves as sinks and near-shore ecosystems as sources of atmospheric CO_2. Deep-Sea Res. II 56 (8–10), 554–577. https://doi.org/10.1016/j.dsr2.2008.12.009.

Chen, C.-T.A., Huang, T.H., Chen, Y.C., et al., 2013. Air-sea exchanges of CO_2 in the world's coastal seas. Biogeosciences 10, 6509–6544. https://doi.org/10.5194/bg-10-6509-2013.

Cole, J.J., Prairie, Y.T., Caraco, N.F., et al., 2007. Plumbing the global carbon cycle: integrating inland waters into the terrestrial carbon budget. Ecosystems 10 (1), 171–184. https://doi.org/10.1007/s10021-006-9013-8.

Crosswell, J.R., Paerl, H.W., Wetz, M.S., et al., 2012. Air-water CO_2 fluxes in the microtidal Neuse River Estuary, North Carolina. J. Geophys. Res. 117 (C08017). https://doi.org/10.1029/2012JC007925.

Crosswell, J.R., Wetz, M.S., Hales, B., et al., 2014. Extensive CO_2 emissions from shallow coastal waters during passage of Hurricane Irene (August 2011) over the Mid-Atlantic Coast of the U.S.A. Limnol. Oceanogr. 59 (5), 1651–1665. https://doi.org/10.4319/lo.2014.59.5.1651.

Crosswell, J.R., Anderson, I.C., Stanhope, J.W., et al., 2017. Carbon budget of a shallow, lagoonal estuary: Transformations and source-sink dynamics along the river-estuary-ocean continuum. Limnol. Oceanogr. https://doi.org/10.1002/lno.10631.

Dahal, D., Liu, S., Oeding, J., 2014. The carbon cycle and Hurricanes in the United States between 1900 and 2011. Sci. Rep. 4, 1–10. https://doi.org/10.1038/srep05197.

Dinauer, A., Mucci, A., 2017. Spatial variability of surface-water pCO_2 and gas exchange in the world's largest semi-enclosed estuarine system: St. Lawrence Estuary (Canada). Biogeosciences 14, 3221–3237. https://doi.org/10.5194/bg-2017-1.

Drupp, P., De Carlo, E.H., Mackenzie, F.T., et al., 2011. Nutrient inputs, phytoplankton response, and CO_2 variations in a semi-enclosed subtropical embayment, Kaneohe Bay, Hawaii. Aquat. Geochem. 17, 473–498. https://doi.org/10.1007/s10498-010-9115-y.

Evans, W., Hales, B., Strutton, P.G., 2012. pCO_2 distributions and air–water CO_2 fluxes in the Columbia River estuary. Estuar. Coast. Shelf Sci. 117, 260–272. https://doi.org/10.1016/j.ecss.2012.12.003.

Fagan, K.E., Mackenzie, F.T., 2007. Air–sea CO_2 exchange in a subtropical estuarine-coral reef system, Kaneohe Bay, Oahu, Hawaii. Mar. Chem. 106, 174–191. https://doi.org/10.1016/j.marchem.2007.01.016.

Hall, N.S., Paerl, H.W., Peierls, B.L., et al., 2012. Effects of climatic variability on phytoplankton community structure and bloom development in the eutrophic, microtidal, New River Estuary, North Carolina, USA. Estuar. Coast. Shelf Sci. 117, 70–82.

Herrmann, M., Najjar, R.G., Kemp, M.W., et al., 2015. Net ecosystem production and organic carbon balance of U.S. East Coast estuaries: a synthesis approach. Glob. Biogeochem. Cycles 29, 96–111. https://doi.org/10.1002/2013GB004736.

Hopkinson, C.S., Vallino, J.J., 1995. The relationships among man's activities in watersheds and estuaries: a model of runoff effects on patterns of estuarine community metabolism. Estuaries 18. https://doi.org/10.2307/1352380.

Hu, X., Cai, W.-J., 2013. Estuarine acidification and minimum buffer zone—a conceptual study. Geophys. Res. Lett. 40 (19), 5176–5181. https://doi.org/10.1002/grl.51000.

Hunt, C.W., Salisbury, J.E., Vandemark, D., et al., 2011. Contrasting carbon dioxide inputs and exchange in three adjacent New England estuaries. Estuar. Coasts 34 (1), 68–77. https://doi.org/10.1007/s12237-010-9299-9.

Hunt, C.W., Salisbury, J.E., Vandemark, D., 2014. CO_2 input dynamics and air–sea exchange in a large New England estuary. Estuar. Coasts 37 (5), 1078–1091. https://doi.org/10.1007/s12237-013-9749-2.

Ito, T., Marshall, J., Follows, M., 2004. What controls the uptake of transient tracers in the Southern Ocean? Global Biogeochemical Cycles 18 (2), 1–17. https://doi.org/10.1029/2003GB002103.

Jeffrey, L.C., Maher, D.T., Santos, I.R., et al., 2016. Groundwater, acid and carbon dioxide dynamics along a Coastal Wetland, Lake and Estuary Continuum. Estuar. Coasts 39 (5), 1325–1344. https://doi.org/10.1007/s12237-016-0099-8.

Jiang, L.-Q., Cai, W.-J., Wang, Y., 2008. A comparative study of carbon dioxide degassing in river- and marine-dominated estuaries. Limnol. Oceanogr. 53, 2603–2625.

Joesoef, A., Huang, W.J., Gao, Y., Cai, W.-J., 2015. Air-water fluxes and sources of carbon dioxide in the Delaware Estuary: Spatial and seasonal variability. Biogeosciences 12 (20), 6085–6101. https://doi.org/10.5194/bg-12-6085-2015.

Joesoef, A., Kirchman, D.L., Sommerfield, C.K., et al., 2017. Seasonal variability of the inorganic carbon system in a large coastal plain estuary. Biogeosciences 14 (21), 4949–4963. https://doi.org/10.5194/bg-14-4949-2017.

Jones, D.C., Ito, T., Takano, Y., Hsu, W.C., 2014. Spatial and seasonal variability of the air-sea equilibration timescale of carbon dioxide. Global Biogeochemical Cycles 28 (11), 1163–1178. https://doi.org/10.1002/2014GB004813.

Kemp, W.M., Smith, E.M., Marvin-Dipasquale, M., et al., 1997. Organic carbon balance and net ecosystem metabolism in Chesapeake Bay. Mar. Ecol. Prog. Ser. 150, 229–248.

Laruelle, G.G., Goossens, N., Arndt, S., et al., 2017. Air-water CO_2 evasion from U.S. East Coast estuaries. Biogeosciences 14, 2441–2468. https://doi.org/10.5194/bg-2016-278.

Lévy, M., Lengaigne, M., Bopp, L., et al., 2012. Contribution of tropical cyclones to the air-sea CO_2 flux: a global view. Glob. Biogeochem. Cycles 26 (2). https://doi.org/10.1029/2011GB004145.

Lewis, E., Wallace, D., 1998. Program Developed for CO_2 System Calculations, ed. C.D.I. A. Center. Oak Ridge, Tennessee: Carbon Dioxide Information Analysis Center.

Li, Y., Yang, X., Han, P., Xue, L., Zhang, L., 2017. Controlling mechanisms of surface partial pressure of CO2 in Jiaozhou Bay during summer and the influence of heavy rain. Journal of Marine Systems 173, 49–59. https://doi.org/10.1016/j.jmarsys.2017.04.006.

Luettich, R.A., Reynolds-Fleming, J.V., McNinch, J.E., et al., 2000. Circulation characteristics of the Neuse River Estuary, North Carolina. http://www.unc.edu/ims/neuse/modmon/publications/circ_ms/Luettich_et_al.pdf (accessed 10 January 2018).

Maher, D.T., Eyre, B.D., 2012. Carbon budgets for three autotrophic Australian estuaries: Implications for global estimates of the coastal air-water CO_2 flux. Glob. Biogeochem. Cycles 26. https://doi.org/10.1029/2011GB004075.

Mallin, M., Paerl, H.W., Rudek, J., et al., 1993. Regulation of estuarine primary production by watershed rainfall and river flow. Mar. Ecol. Prog. Ser. 93, 199–203. https://doi.org/10.3354/meps093199.

Mallin, M.A., McIver, M.R., Wells, H.A., et al., 2005. Reversal of eutrophication following sewage treatment upgrades in the New River Estuary, North Carolina. Estuaries 28 (5), 750–760. https://doi.org/10.1007/BF02732912.

Millero, F.J., 2010. Carbonate constants for estuarine waters. Mar. Freshw. Res. 61, 139–142. https://doi.org/10.1071/MF09254.

Mørk, E.T., Sejr, M., Stæhr, P.A., et al., 2016. Temporal variability of air-sea CO_2 exchange in a low-emission estuary. Estuar. Coast. Shelf Sci. 176, 1–11. https://doi.org/10.1016/j.ecss.2016.03.022.

Osburn, C.L., Handsel, L., Mikan, M., et al., 2012. Fluorescence tracking of dissolved and particulate organic matter quality in a river- dominated estuary system. Environ. Sci. Technol. 46, 8628–8636. https://doi.org/10.1021/es3007723.

Paerl, H.W., Pinckney, J., Fear, J., et al., 1998. Ecosystem responses to internal and watershed organic matter loading: consequences for hypoxia in the eutrophying Neuse River Estuary, North Carolina, USA. Mar. Ecol. Prog. Ser. 166, 17–25. https://doi.org/10.3354/meps166017.

Paerl, H.W., Valdes, L.M., Joyner, A.R., et al., 2006a. Ecological response to hurricane events in the Pamlico Sound system, North Carolina, and implications for assessment and management in a regime of increased frequency. Estuar. Coasts 29 (6), 1033–1045. https://doi.org/10.1007/BF02798666.

Paerl, H.W., Valdes, L.M., Peierls, B.L., et al., 2006b. Anthropogenic and climatic influences on the eutrophication of large estuarine ecosystems. Limnol. Oceanogr. 51, 448–462. https://doi.org/10.4319/lo.2006.51.1_part_2.0448.

Paerl, H.W., Crosswell, J.R., Van Dam, B., Hall, N.S., Rossignol, K.L., Osburn, C.L., Hounshell, A.G., Sloup, R.S., Harding, L.W., 2018. Two decades of tropical cyclone impacts on North Carolina's estuarine carbon, nutrient and phytoplankton dynamics: Implications for biogeochemical cycling and water quality in a stormier world. Biogeochemistry. https://doi.org/10.1007/s10533-018-0438-x.

Peierls, B.L., Hall, N.S., Paerl, H.W., 2012. Non-monotonic responses of phytoplankton biomass accumulation to hydrologic variability: a comparison of two coastal plain North Carolina estuaries. Estuar. Coasts 35 (6), 1376–1392. https://doi.org/10.1007/s12237-012-9547-2.

Reynolds-Fleming, J.V., Fleming, J.G., Luettich, R.A., 2002. Portable, autonomous vertical profiler for estuarine applications. Estuaries 25 (1), 142–147. https://doi.org/10.1007/BF02696058.

Ruiz-Halpern, S., Maher, D.T., Santos, I.R., et al., 2015. High CO_2 evasion during floods in an Australian subtropical estuary downstream from a modified acidic floodplain wetland. Limnol. Oceanogr. 60, 42–56. https://doi.org/10.1002/lno.10004.

Sarma, V.S., Kumar, N.A., Prasad, V.R., et al., 2011. High CO_2 emissions from the tropical Godavari estuary (India) associated with monsoon river discharges. Geophys. Res. Lett. 38 (8). https://doi.org/10.1029/2011GL046928.

Takahashi, T., Olafsson, J., Goddard, J.G., et al., 1993. Seasonal variation of CO_2 and nutrients in the high latitude surface ocean: a comparative study. Glob. Biogeochem. Cycles 7, 843–878.

Takahashi, T., Sutherland, S.C., Sweeney, C., et al., 2002. Global sea—air CO_2 flux based on climatological surface ocean pCO_2, and seasonal biological and temperature effects. Deep-Sea Res. II Top. Stud. Oceanogr. 49, 1601–1622. https://doi.org/10.1016/S0967-0645(02)00003-6.

Van Dam, B.R., Crosswell, J.R., Anderson, I.C., et al., 2018. Watershed-scale drivers of air-water CO_2 exchanges in two lagoonal, North Carolina (USA) estuaries. J. Geophys. Res. Biogeosci. 123. https://doi.org/10.1002/2017JG004243.

Weiss, R.F., 1974. Carbon dioxide in water and seawater: the solubility of a non-ideal gas. Mar. Chem. 2, 203–215.

Wetz, M.S., Yoskowitz, D.W., 2013. An “extreme” future for estuaries? Effects of extreme climatic events on estuarine water quality and ecology. Mar. Pollut. Bull. 69, 7–18. https://doi.org/10.1016/j.marpolbul.2013.01.020.

Yao, H., Hu, X., 2017. Responses of carbonate system and CO_2 flux to extended drought and intense flooding in a semiarid subtropical estuary. Limnol. Oceanogr. https://doi.org/10.1002/lno.10646.

Ye, H., Sheng, J., Tang, D., et al., 2017. Storm-induced changes in pCO_2 at the sea surface over the northern South China Sea during Typhoon Wutip. J. Geophys. Res. Oceans 122, 2050–2068. https://doi.org/10.1002/2016JC012115.

Zscheischler, J., Mahecha, M.D., Avitabile, V., et al., 2017. Reviews and syntheses: an empirical spatiotemporal description of the global surface—atmosphere carbon fluxes: opportunities and data limitations. Biogeosciences 14, 3685–3703. https://doi.org/10.5194/bg-14-3685-2017.